

GENERALIZED CRITICAL CURRENT DENSITY OF COMMERCIAL Nb46.5, Nb50  
AND Nb53 w/o Ti MULTIFILAMENTARY SUPERCONDUCTORS

K. F. Hwang\* and D. C. Larbalestier

ABSTRACT

We have measured the critical current density  $J_c$  of four different commercial compositions of NbTi over the range of fields up to  $H_2$  and at reduced temperatures. We have presented the results in scaled form so that attainable values of  $J_c$  in NbTi at arbitrary fields and temperatures may easily be derived. We have also measured the effect of post manufacture thermal treatments on  $J_c$  and shown that the change in  $J_c$  scales with a temperature compensated time factor.

INTRODUCTION

NbTi alloys are still the most widely used superconducting alloys and high critical current densities can be obtained over a range of alloy contents. To a certain extent different alloy compositions have become standard in different countries, e.g. Nb44 w/o Ti in Britain, Nb46.5 w/o Ti in the U.S.A. and Nb50 w/o Ti in Germany. All of these alloy compositions are capable of giving  $J_c > 1700 \text{ A/mm}^2$  at 5 T and 4.2 K. However, it has also been reported that values twice as large as these can be obtained from Nb50 Ti when properly optimized. For superconducting magnetic energy storage (SMES) applications NbTi is one of the two major determinants of the storage cost and we have therefore been studying the possibilities and characteristics of high  $J_c$  NbTi alloys of different composition with particular interest. In this paper we report on the critical current properties of four different commercial alloys, of nominal compositions Nb46.5, Nb50 (2) and Nb53 w/o Ti at fields from 0 to  $H_{c2}$ , both at 4.2 K and at reduced temperatures.

A common microstructural feature of each of these compositions is that they all possess a high dislocation density ( $\sim 10^{12} \text{ cm/cm}^3$ ) and that these dislocation arrangements are of decisive importance in determining  $J_c$ . At some stages, typically within 4-6 times the final wire diameter and at the final wire size, the manufacturer gives controlled heat treatments to the wire, the effect of which are to constructively modify the dislocation distribution and possibly encourage a precipitation reaction. The high dislocation densities are, however, thermally unstable and their sensitivity to the exact heat input of the thermal treatment is probably the cause of the greater part of the batch to batch scatter in  $J_c$  seen in producing nominally identical billets of superconductor. In large magnet systems there may, in addition, be post delivery heat inputs reaching the NbTi and we have followed the response of these alloys to post production heat treatments partly to establish safe limits for such inputs and partly to give us

fundamental information about the role of microstructure in determining  $J_c$ . A preliminary report of this work for Nb46.5 w/o Ti has already appeared.

EXPERIMENTAL PROCEDURE

Four wires were studied of nominal composition Nb46.5 Ti (MCA), Nb53 Ti (Airco) together with two samples of Nb50 Ti (Vacuumschmelze). This range covers a composition in which few  $\alpha$ -Ti precipitates are found (Nb46.5 Ti), a composition, Nb50 Ti, in which they can be finely dispersed and extremely effective<sup>1,6</sup> and a composition, Nb53 Ti in which they can form rather easily, permitting high  $J_c$  with less cold work than is needed for the lower Ti alloys. Other details of the composites are given in Table 1. Alloy compositions of the Nb 50 and Nb53 Ti alloys were determined by electron probe microanalysis against calibrated standards. The tolerance on the Nb46.5 w/o Ti is stated to be  $\pm 1.5 \text{ w/o Ti}$ .

TABLE I  
Sample Specifications

Manufacturer	Nb46.5 w/o Ti MCA	Nb49.7 w/o Ti Vacuumschmelze	Nb50.4 w/o Ti Vacuumschmelze	Nb52.7 w/o Ti Airco
Wire diameter (mm)	0.686	0.629	0.600	0.831
Copper/S.C. ratio	1.8:1	1.7:1	1.2:1	1.8:1
Number of filaments	2100	2000	60	180
Filament size ( $\mu\text{m}$ )	10	9	52	38

Critical current measurements were made using standard techniques. Penetration lengths in these composites are small ( $< 1 \text{ cm}$ ) and approximately 20 cm long hairpin samples were used, ensuring negligible current transfer voltages. Measurements up to 7 tesla were made in Madison, those above 7 T and below 4.2 K at the National Magnet Laboratory, MIT. The criterion for  $I_c$  in each case was the appearance of a voltage of  $1 \mu\text{V/cm}$ . Voltage tap separation was  $\sim 5 \text{ cm}$  in Madison and  $\sim 3 \text{ cm}$  at MIT. Heat treatments were carried out in evacuated silica capsules contained 1/3 atm. of argon in furnaces whose constant temperature zone ( $\pm 5^\circ\text{C}$ ) considerably exceeded the voltage tap separation.

RESULTS AND DISCUSSION

Figure 1 shows the critical current density vs. magnetic field at 4.2 K for the four alloys studied. Note the considerable range of values obtained, from  $1700 \text{ A/mm}^2$  to  $2700 \text{ A/mm}^2$  at 5 tesla and in particular the fact that the two nominal Nb50 Ti samples had widely different  $J_c$  values. That for the smaller filament Nb49.7 w/o Ti had a  $J_c$  of  $1850 \text{ A/mm}^2$  at 5 T while the Nb50.4 w/o Ti had the much higher figure of  $2700 \text{ A/mm}^2$  even though the filament size exceeded  $50 \mu\text{m}$ . At present the commercial state of the art is about  $1800\text{--}2000 \text{ A/mm}^2$  at 5 T so that the high values exhibited by the 50.4 Ti alloy are of considerable interest. At present we are examining

Manuscript received September 28, 1978.

\*Engineering Experiment Station, Univ. of Wisconsin, 1500 Johnson Drive, Madison, Wisconsin 53706.

the microstructure of these alloys using transmission electron microscopy but our studies are not yet complete. While we know that precipitates are present in all the alloys we do not yet know their detailed distribution although we may surmise that in the Nb50.4 w/o Ti the thermal and mechanical processing schedule has been such as to produce a fine distribution of normal  $\alpha$ -Ti precipitates within the dislocation cell structure.<sup>1,6</sup>

The gains in  $J_c$  to be made on going to temperatures lower than 4.2 K are well known in principle, and  $J_c$  curves for Nb50.4 w/o Ti at lower temperatures are shown in Fig. 2. Note that there is a 45% increase in  $J_c$  at 5 T on going from 4.2 to 2.5 K.  $H_{c2}$  is seen to scale as  $T^2$  over this range increasing from about 10.8 tesla at 4.2 K to about 15 tesla at 0°K (Fig. 3). In the superfluid He range ( $< 2.17$  K)  $H_{c2}$  attains values of 13.8 tesla and above. If we arbitrarily take a current density of 250 A/mm<sup>2</sup> as a lower useful limit, we see this is attained at about 1-1.5 tesla below  $H_{c2}$ , suggesting that NbTi may be useful in magnetic fields up to 12.5 tesla in magnets cooled by superfluid helium. There are also advantages for lower field use. For 3 tesla superconducting magnetic energy storage units operated at 1.8-2 K the approximately two-fold increase in  $J_c$  in the NbTi and the greatly enhanced heat transfer obtained from superfluid helium more than offset the increased refrigeration cost.

A useful way of presenting the reduced temperature data in parametric form is to plot the bulk pinning force ( $F_p = J_c \times B$  A.T. m<sup>-2</sup> = N.m<sup>-3</sup>) vs. field (Fig. 4). The pinning force curve is seen to come to a characteristic maximum at about  $1/2 H_{c2}$ . If the reduced parameters  $F_p/F_{pmax}$  vs.  $H/H_{c2}$  are plotted, it is seen that one universal curve is obtained for each alloy. Such scaling curves have been shown to be a general feature of hard type II superconductors.<sup>8</sup> A useful consequence of the scaling is that if the temperature variation of  $F_{pmax}$  and  $H_{c2}$  is also known then the critical current density at any arbitrary field and temperature can be read from the scaling law curve. Scaling curves for each of the four alloys are given in Figs. 5-8 and the variation of  $H_{c2}$  and  $F_{pmax}$  with temperature in Figs. 3 and 9.

Heat treatments were carried out between 275 and 500°C. Here we report on the effects of the 300-500°C heat treatments for the three higher Ti content alloys, those on the Nb46.5 Ti alloy having already been reported.<sup>9</sup> In the range 300-500°C the effect of the post production heat treatment is to reduce the  $J_c$ , indicating that the manufacturers' schedules were either close to optimum or over optimum (in each case the as-received  $J_c$  values were good by comparison with industry standards). Several hours at 300°C do not reduce  $J_c$  by much (5-10% maximum) so that clearly there is little to fear from immersing conductors in Pb-Sn or Sn-Ag solder baths. On the other hand, temperatures of 500°C and above produce rapid degradation in  $J_c$  and are not tolerable so that for example casting high purity Al (MP = 660°C) around NbTi, although desirable in principle, does not appear feasible in practice. The effect of heat treatments between 300 and 500°C can also be scaled, as is demonstrated in Fig. 13 where the fractional decrease

in  $J_c$  with heat treatment as a function of the temperature compensated time is plotted. The temperature (T) compensated time (t) is  $t \exp(-E_a/kT)$  where  $E_a$  is the activation energy associated with the microstructural process controlling the change in  $J_c$  and k is Boltzmann's constant. We defer a fuller discussion of the significance of the derived activation energies until a later date. It is, however, interesting to note that the spread in  $E_a$  observed (2.4-1.8 eV) is rather large for such a narrow composition range and may be an important reason why the manufacturers' heat treatments produce the spread in  $J_c$  that they do.

Large scale copies of the graphs may be obtained directly from the authors for those who wish to scale in detail from them.

#### ACKNOWLEDGEMENTS

We are grateful to Dr. Bruce P. Strauss for one of the samples of NbTi, to Dr. Anne West for some preliminary electron microscopy results, to Prof. R.W. Boom for continued encouragement, and to Min-Hwa Chi, David Hawksworth and Robert Rensbottom for much experimental assistance. We are also pleased to acknowledge the use of the high field magnet facilities at the National Magnet Laboratory, MIT.

#### REFERENCES

1. J. Willbrand and W. Schlump, Z. Metallk., Vol. 66 (12), pp. 714-19, 1975.
2. R.W. Boom et al., "Wisconsin Superconductive Energy Storage Project," 1976 Annual Report, May, 1977.
3. B.P. Strauss, R.H. Rensbottom, and R.H. Flora, Proceedings of the 7th Symposium on Engineering Problems of Fusion Research, Vol. II, pp. 1271-72 Knoxville, Tenn., 1977.
4. B.P. Strauss, Fermilab, private communication.
5. D.C. Larbalestier, R. Flach, D.G. Hawksworth, Proceedings of 6th International Conference on Magnet Technology (MI-6), Bratislava, Czechoslovakia, Vol. 1, pp. 1076, August 1977.
6. I. Pfeiffer and H. Hillman, Acta Met. Vol. 16, pp. 1249, 1968.
7. S.W. Van Sciver, pp. 694, Ref. 3.
8. E.J. Kramer, J. Appl. Phys., Vol. 44, pp. 1360, 1973.

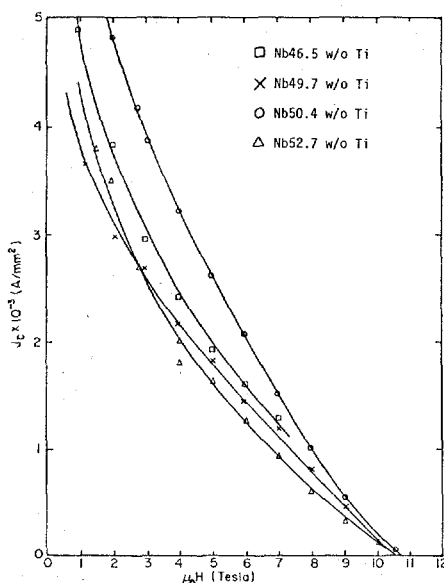


Fig. 1. Critical current density vs. field at 4.2 K.

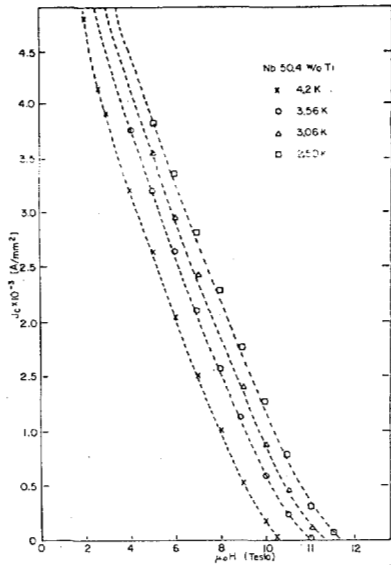


Fig. 2. Critical current density vs. field for Nb50.4 w/o Ti at reduced temperature.

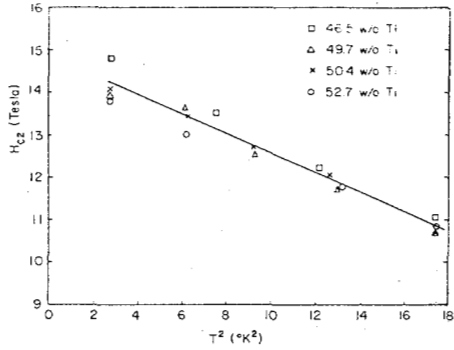


Fig. 3. Upper critical field vs.  $T^2$  for various samples.

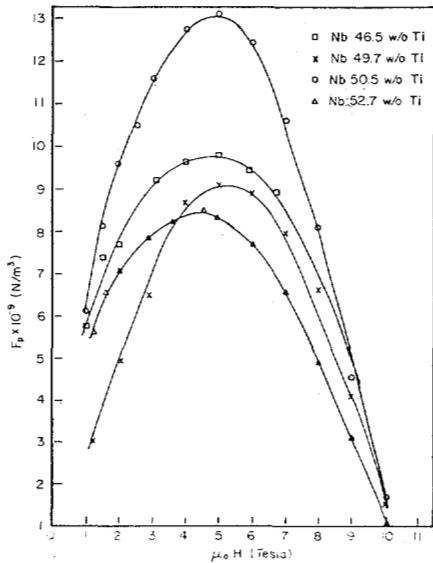


Fig. 4. Pinning force density ( $J_c \times B$ ) vs. field at 4.2 K.

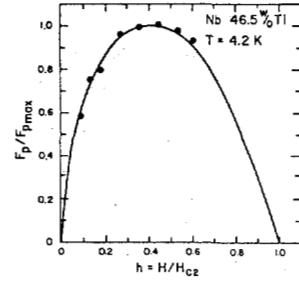


Fig. 5. Normalized pinning force vs. reduced field for Nb46.5 Ti at 4.2 K.

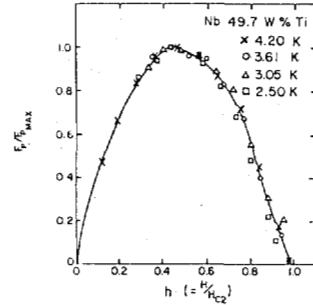


Fig. 6. Normalized pinning force density for Nb49.7 w/o Ti at various temperatures.

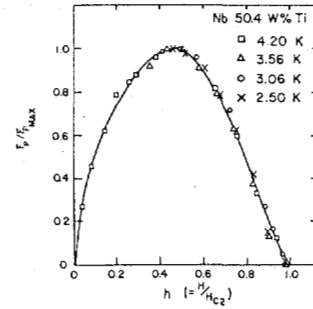


Fig. 7. Normalized pinning force density for Nb50.4 w/o Ti.

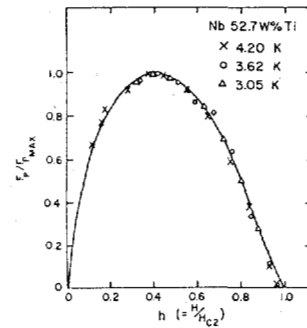


Fig. 8. Normalized pinning force for Nb52.7 w/o Ti.

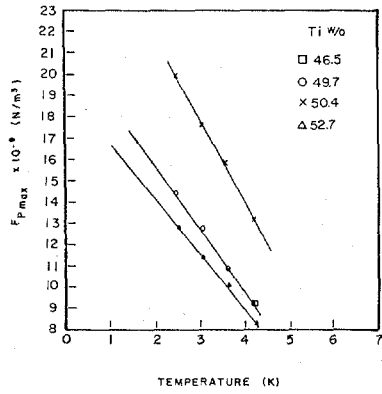


Fig. 9. Maximum pinning force density as a function of temperature.

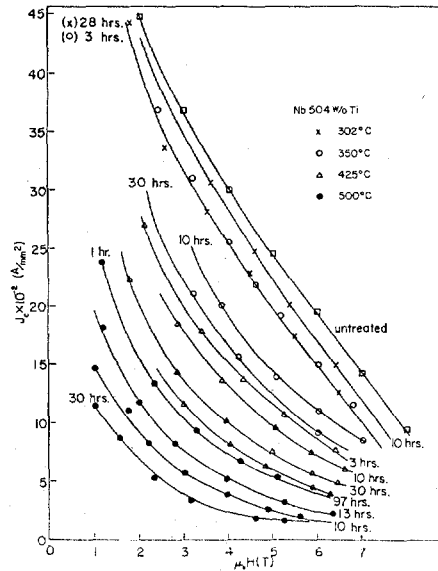


Fig. 11. Critical current density of Nb50.4 w/o Ti at various heat treatments.

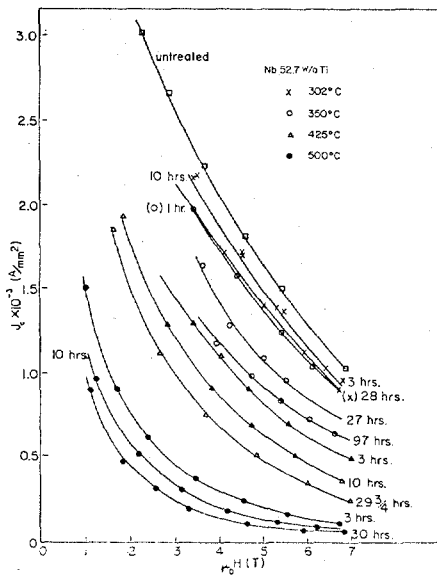


Fig. 10. Critical current density vs. field at various heat treatment conditions for Nb52.7 w/o Ti.

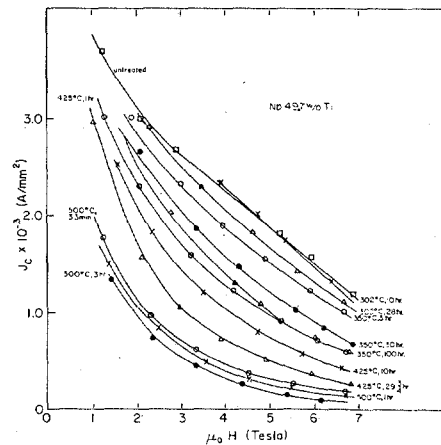


Fig. 12. Critical current density of Nb49.7 w/o Ti at various heat treatments.

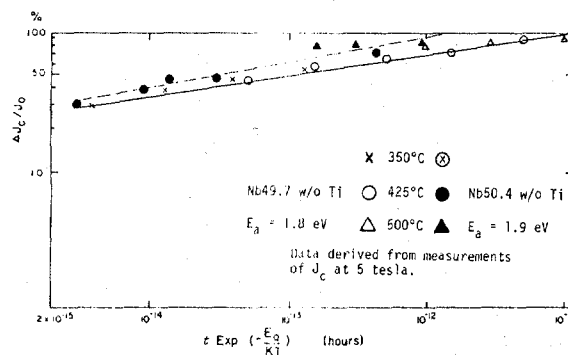


Fig. 13. Fractional decrease of  $J_c$  resulting from heat treatment as a function of treatment time and temperature.